HbtR, a heterofunctional homolog of the virulence regulator TcpP, facilitates the transition between symbiotic and planktonic lifestyles in *Vibrio fischeri*.

Brittany D. Bennett, Tara Essock-Burns, and Edward G. Ruby

Pacific Biosciences Research Center, University of Hawai‘i—Manoa, Honolulu, HI 96813

Running head: Regulation of lifestyle transition in *V. fischeri*

Address correspondence: eruby@hawaii.edu

Abstract

The bioluminescent bacterium *Vibrio fischeri* forms a mutually beneficial symbiosis with the Hawaiian bobtail squid, *Euprymna scolopes*, in which the bacteria, housed inside a specialized light organ, produce light used by the squid in its nocturnal activities. Upon hatching, *E. scolopes* juveniles acquire *V. fischeri* from the seawater through a complex process that requires, among other factors, chemotaxis by the bacteria along a gradient of *N*-acetylated sugars into the crypts of the light organ, the niche in which the bacteria reside. Once inside the light organ, *V. fischeri* transitions into a symbiotic, sessile state in which the quorum-signaling regulator LitR induces luminescence. In this work we show that expression of *litR* and luminescence are repressed by a homolog of the *V. cholerae* virulence factor TcpP, which we have named HbtR. Further, we demonstrate that LitR represses genes involved in motility and chemotaxis into the light organ and activates genes required for exopolysaccharide production.

Importance

TcpP homologs are widespread throughout the *Vibrio* genus; however, the only protein in this family described thus far is a *V. cholerae* virulence regulator. Here we show that HbtR, the TcpP homolog in *V. fischeri*, has both a biological role and regulatory pathway completely unlike that in *V. cholerae*. Through its repression of the quorum-signaling regulator LitR, HbtR affects the expression of genes important for colonization of the *E. scolopes* light organ. While LitR becomes activated within the crypts, and upregulates luminescence and exopolysaccharide genes and downregulates chemotaxis and motility genes, it appears that HbtR, upon expulsion of *V. fischeri* cells into seawater, reverses this process to aid the switch from a symbiotic to a planktonic state. The

possible importance of HbtR to the survival of *V. fischeri* outside of its animal host may have broader implications for the ways in which bacteria transition between often vastly different environmental niches.

Introduction

The Gram-negative bacterium *Vibrio (Aliivibrio) fischeri* is a model for the study of biochemical processes underpinning bioluminescence, quorum sensing, and bacterial-animal symbioses. Luminescence in *V. fischeri* is activated by a quorum-sensing pathway that responds to high concentrations of two autoinducer molecules, *N*-(3-oxohexanoyl)-L-homoserine lactone (3-oxo-C6-HSL (1)) and *N*-octanoyl-L-homoserine lactone (C8-HSL (2)). When *V. fischeri* cells multiply to a certain density, C8-HSL and 3-oxo-C6-HSL accumulate to high local concentrations, initiating a signaling cascade that leads to upregulation of the regulator LuxR by the regulator LitR and consequent activation of the luciferase operon, *luxICDABEG* (3–5); reviewed in (6).

Light production by *V. fischeri* is a crucial factor in the mutualistic symbiosis it forms within the light organ of the Hawaiian bobtail squid, *Euprymna scolopes* (7–9). Juvenile *E. scolopes* become colonized with *V. fischeri* shortly after hatching into seawater containing this bacterium (10). *V. fischeri* cells initiate light-organ colonization through a series of steps, including chemotaxis towards *N*-acetylated sugars released by the squid (11, 12). After initial colonization of the squid light organ, the symbiosis undergoes a daily cyclic rhythm of three basic stages for the remainder of the squid's life: during the day, *V. fischeri* cells grow to a high density in the crypts on carbon sources provided by the squid (13, 14); at night, the bacteria produce light that aids in

camouflage for the squid (15, 16); and at dawn, ~95% of the bacterial cells are expelled from the light organ into the seawater, where they may initiate colonization of new squid hatchlings, while the remaining ~5% repopulate the light organ (17, 18).

Previous work indicated that, in *V. fischeri* cells newly expelled from the light organ, numerous genes are up- and downregulated relative to their level of expression in planktonic cells (19). Two of the genes upregulated in expelled cells were VF_A0473 and VF_A0474, comprising a small operon annotated as encoding homologs of the genetic regulator TcpP and its chaperone, TcpH. TcpP was first described in *V. cholerae* as a virulence gene regulator (20, 21). During the early stages of *V. cholerae* infection, TcpP works synergistically with another transcriptional regulator, ToxR, to upregulate expression of the virulence regulator *toxT* and thereby activate expression of cholera toxin and the toxin-coregulated pilus in response to changing environmental conditions (21, 22). *tcpPH* expression is itself induced by AphA and AphB in response to low oxygen or acidic pH (23–25). In *V. cholerae* El Tor biotypes, *aphA* expression is repressed by HapR (the *V. cholerae* ortholog of LitR) upon initiation of quorum sensing at high cell densities (26, 27). Additionally, activation of *tcpPH* expression by AphA and AphB is inhibited by the global metabolic regulator Crp (28). This complex regulatory pathway serves to upregulate *tcpPH* and, consequently, downstream virulence factors under conditions consistent with entry into the vertebrate gut, a process reversed late in the infection cycle before the bacteria exit the host and re-enter an aquatic environment (29, 30).

No published genomes of *V. fischeri* strains encode homologs of either *toxT* or cholera toxin genes. The genome of the model strain *V. fischeri* ES114 does encode

annotated homologs of the toxin-coregulated pilus genes *tcpFETSD* and *tcpCQBA*, but this strain is alone among the 66 currently available *V. fischeri* genomes to do so. The *V. fischeri* genes regulated by the protein product of VF_A0473 are therefore unknown, as are any upstream regulatory factors that determine under which conditions the regulator is produced and active. Here we present evidence that VF_A0473 regulates genes governing phenotypes relevant to the switch from symbiosis to a planktonic lifestyle. We therefore rename VF_A0473 and VF_A0474, currently annotated as *tcpP* and *tcpH*, as *hbtR* (*h*a*b*itat *t*ransition *r*egulator) and *hbtC* (*h*a*b*itat *t*ransition *c*haperone). In this work, we identify the HbtR regulon and uncover aspects of *hbtRC* regulation. Further, we determine that LitR is repressed by HbtR and describe LitR-regulated phenotypes beyond luminescence that are important for light-organ colonization.

Results

<u>The HbtR regulon is distinct from that of TcpP.</u> Considering that *V. fischeri* and *V. cholerae* have significantly different lifestyles, as well as the absence in 65 of 66 sequenced *V. fischeri* genomes of homologs of virulence-factor genes regulated by TcpP in *V. cholerae*, we postulated that HbtR has a distinct function from that of TcpP. To determine the regulon of HbtR, RNA-seq was performed using Δ*hbtRC* mutant strains of *V. fischeri* ES114 carrying either empty vector or an inducible vector with *hbtRC* under control of the *lac* promoter. Notable among the RNA-seq results (Table S1 Excel file) is that none of the *tcp* pilus gene homologs encoded in the *V. fischeri* ES114 genome were expressed at significantly different levels in *hbtRC* strains carrying either

empty vector or the inducible *hbtRC* vector (Table S1), ruling out the possibility that HbtR regulates the same genes in *V. fischeri* ES114 as TcpP does in *V. cholerae*.

HbtR represses *litR* expression and luminescence *in vitro*. Among the genes significantly downregulated in the RNA-seq results when *hbtRC* was expressed were the quorum signaling-regulated genes *litR*, *luxR*, *qsrP*, and *rpoQ* (Table S1). Less strongly, but statistically significantly, downregulated genes included most of the luciferase operon (Table S1). To determine whether repression of *lux* genes by HbtR affects bacterial light emission, luminescence and growth were monitored in cultures of wild-type *V. fischeri* and its Δ*hbtRC* derivative carrying either empty vector or vector constitutively expressing *hbtRC*. Deletion of *hbtRC* did not affect light production; however, overexpression of *hbtRC* in either wild type or Δ*hbtRC* led to a delay in onset and significant decrease in intensity of light production (Fig. 1A). There was no difference in growth rate between the strains (Fig. 1B), eliminating the possibility that the reduced luminescence by the *hbtRC*-overexpression strains was due to a growth defect. To determine whether deletion or overexpression of *hbtRC* would lead to a change in light production by *V. fischeri* within the light organ, *E. scolopes* hatchlings were colonized with wild-type *V. fischeri* or Δ*hbtRC*. There was no difference in the luminescence of juvenile squid colonized by any *V. fischeri* strains at either 24 or 48 h (Fig. S1), suggesting that HbtR is not active inside the light organ.

HbtR activates and LitR represses chemosensory genes involved in *E. scolopes* light-organ colonization. Among the genes upregulated in the *hbtRC*-expressing strain in the

RNA-seq experiment were four genes annotated as encoding methyl-accepting chemotaxis proteins (MCPs): VF_1133, VF_2042, VF_A0246, and VF_A0389 (Table S1). To confirm that the upregulation of these MCP genes by HbtR functions through its repression of *litR* expression, RT-qPCR was performed on wild-type *V. fischeri* and Δ*litR*. Expression of all four of these MCP genes was significantly increased in Δ*litR* compared to wild-type *V. fischeri* (Table 1).

As chemotaxis is essential to colonization of the *E. scolopes* light organ by *V. fischeri* (12), we asked whether any of the four MCPs repressed by LitR are involved in colonization. Newly hatched *E. scolopes* juveniles were exposed to a 1:1 ratio of wild-type *V. fischeri* and a quadruple mutant with in-frame deletions of all four of the LitR-repressed MCP genes (ΔVF_1133ΔVF_2042ΔVF_A0246ΔVF_A0389; "ΔΔΔΔ"). Regardless of which strain carried a *gfp*-labeled plasmid, the squid light organ populations tended to be dominated by wild-type *V. fischeri* (Fig. 2), indicating that HbtR and LitR regulate chemotaxis genes involved in initiating symbiosis.

To determine whether the colonization defect displayed by ΔΔΔΔ is due to the chemosensory function of any of the four MCP genes, we sought to identify the chemoattractants recognized by these MCPs. Wild-type *V. fischeri* and MCP deletion mutants were spotted onto minimal-medium, soft-agar plates containing 1 mM of three known chemoattractants for *V. fischeri* (12): *N*-acetyl-D-glucosamine (GlcNAc), *N*,*N′*-diacetylchitobiose ($(GlcNAc)_2$), or *N*-acetylneuraminic acid (Neu5Ac). The chemotactic zone sizes for ΔVF_1133 and ΔVF_A0246 were significantly smaller than wild-type *V. fischeri* on each of the *N*-acetylated sugars (Table 2). There was no significant difference in zone sizes between ΔΔΔΔ and wild-type *V. fischeri* spotted onto plates

containing either no chemoattractant or 1 mM glucose (Table 2), indicating these mutations do not affect motility, or chemotaxis in general. Because they grew equally well on either GlcNAc or Neu5AC (Fig. S2), the differences in zone sizes of the MCP mutants and wild-type *V. fischeri* were unlikely to be growth-related.

HbtR activates and LitR represses motility. Two flagellin genes, *flaC* and *flaF*, were upregulated by *hbtRC* (Table S1), indicating the possible activation of motility by HbtR. An earlier study demonstrated that LitR represses motility in *V. fischeri* (31), and microarrays performed previously (Studer, Schaefer, and Ruby; Schaefer and Ruby unpublished data) indicated that AinS and LitR downregulate the expression of a majority of the flagellin genes within in the locus VF_1836–77, as well as *flaF*, *fliL2*, *motX*, *motA1B1*, and *cheW*. To confirm the repression of motility genes by LitR, RT-qPCR was employed to determine the level of expression of three flagellin or motor genes in different genomic regions in wild-type *V. fischeri* and Δ*litR*. Expression of *cheW*, *motA1*, *flaC*, and *flaF* was moderately, but statistically significantly, higher in Δ*litR* than in wild-type *V. fischeri* (Table 1). However, we were not able to determine the mechanism by which LitR represses multiple motility gene loci, as expression levels of the known flagellin regulatory genes *rpoN*, *flrA*, *flrB*, *fliA*, and *flgM* were comparable between Δ*litR* and wild-type *V. fischeri* strains (Table 1).

The sigma factor-like regulator RpoQ, which is upregulated by LitR, represses motility and/or chemotaxis towards GlcNAc when overexpressed (32). Thus, we wanted to determine whether the effect LitR has on motility and *N*-acetylated sugar chemotaxis is mediated through its regulation of *rpoQ*. On soft-agar chemotaxis plates containing no

chemoattractant or 1 mM GlcNAc, we observed the same pattern regardless of the presence of GlcNAc: either deletion of *litR* or overexpression of *hbtRC* led to larger migration zones than for wild-type *V. fischeri*, while overexpression of *litR* essentially eliminated bacterial migration (Table 2). There were no significant differences between Δ*rpoQ* and wild-type *V. fischeri* strains carrying any vector (Table 2), indicating that the repression of motility by LitR is not mediated through RpoQ.

<u>HbtR represses and LitR activates exopolysaccharide production</u>. An approximately 25-kb locus constituting the genes VF_0157–80 was downregulated when *hbtRC* was expressed (Table S1). Previously performed microarrays indicated that most of the genes in this locus (VF_0159 and VF0162–0180) are also upregulated by AinS and LitR (Studer, Schaefer, and Ruby; Schaefer and Ruby, unpublished data). To confirm the upregulation of this locus by LitR, RT-qPCR was used to evaluate the expression of three genes, located in separate operons, in Δ*litR* and wild-type *V. fischeri*. Expression of VF_0157 (*wbfB*), VF_0164 (*etp*), and VF_0165 (*wzc*) was significantly higher in wild-type *V. fischeri* than in Δ*litR* (Table 1).

Most of the genes in the locus VF_0157–80 are annotated as being involved in production of extracellular polysaccharides. However, gene annotation alone could not indicate which component(s) of the cell envelope (lipopolysaccharide O-antigen, capsule, or exopolysaccharide (EPS)) might be affected by the genes in this locus. To determine which polysaccharide type is produced by the enzymes encoded in VF_0157–80, alcian blue staining was used to detect negatively charged polysaccharides in the supernatants of liquid cultures of *V. fischeri* strains. Both Δ*litR*

and ΔVF0157–80 produced less alcian blue-staining EPS than wild-type *V. fischeri* (Fig. 3A). Overexpression of *litR* in ΔVF0157–80 did not complement the reduction in EPS produced by that mutant (Fig. 3), indicating that essentially all EPS is produced by this locus.

hbtRC expression is regulated by Crp, but not by AphB or quorum sensing. To determine whether *hbtRC* expression in *V. fischeri* is affected by quorum sensing and/or Crp, a regulator known to affect *tcpPH* expression in *V. cholerae*, RT-qPCR was performed on wild-type *V. fischeri*, Δ*litR*, and Δ*crp* grown to OD_{600} ~0.3 and ~1.0. Expression of *hbtRC* was lower at high cell density than at low cell density for all three strains, with no difference between wild-type *V. fischeri* and Δ*litR* at either higher or lower OD_{600} (Table 1). Expression of *hbtRC* in Δ*crp* was below that in wild-type *V. fischeri* at low OD_{600}, but comparable at high OD_{600}. Crp thus appears to activate *hbtRC* expression, the reverse of *tcpPH* regulation by Crp in *V. cholerae*.

Because Crp activates quorum-signaling genes in the *V. fischeri* genome (33), (34), we asked whether quorum signaling is responsible for the change in *hbtRC* expression at different culture densities, and whether this regulation explains the lower expression in the Δ*crp* mutant. The RT-qPCR experiment was repeated for wild-type *V. fischeri* grown in SWT with or without added autoinducers. *hbtRC* expression remained higher at lower cell density in the presence of both autoinducers (Table 1), indicating that quorum signaling is not involved in Crp- and cell density-mediated *hbtRC* regulation.

To determine whether the regulator AphAB and/or a change in pH affect *hbtRC* expression in *V. fischeri*, RT-qPCR was performed on RNA extracted from cultures of wild-type or Δ*aphB V. fischeri* grown at pH 5.5 or 8.5. There was no significant difference in *hbtRC* expression between any of the conditions (Table 1).

<u>*tcpPH* homologs do not cross-complement between *V. fischeri* and *V. cholerae*</u>. Δ*tcpPH* and Δ*hbtRC* strains of *V. cholerae* and *V. fischeri*, respectively, were complemented with empty vector, vector expressing *tcpPH*, or vector expressing *hbtRC*. RT-qPCR was performed on RNA extracted from cultures of each strain to determine the level of *toxT* expression in the *V. cholerae* strains or *litR* expression in the *V. fischeri* strains. While expression of each *tcpPH* homolog complemented the respective deletion, cross-complementation had no effect on output gene expression (Table 1), illustrating the divergent activities of HbtR and TcpP.

In *V. cholerae*, ToxR cooperates with TcpP to activate *toxT* expression (35, 36), begging the question of whether ToxR is also involved in controlling the *V. fischeri* HbtR regulon. RT-qPCR performed on RNA extracted from cultures of Δ*hbtRC* and Δ*hbtRC*Δ*toxRS* carrying either empty vector or vector expressing *hbtRC* showed that *litR* expression was repressed to the same degree by HbtR regardless of the presence or absence of *toxRS* (Table 1), further demonstrating that regulation by HbtR differs substantially from the TcpP system.

<u>Δ*hbtRC* has no defect in colonizing juvenile *E. scolopes* light organs.</u> Previous work indicated that Δ*hbtRC* (then referred to as Δ*tcpPH*) had a light-organ colonization

defect, which appeared to increase through 96 h (19). We replicated this defect when using the same conditions as the previous study (Fig. 4A); however, we observed an advantage for Δ*hbtRC* when we reversed the fluorescent marker plasmids (Fig. 4B), indicating the earlier results were due simply to experimental design. Co-colonization of juvenile *E. scolopes* with chromosomally labeled strains resulted in no significant colonization defect for any strain (Fig. 4C), demonstrating that HbtR is in fact not required for entry into, or life inside, the *E. scolopes* light organ. Based on this experience, we urge caution by other researchers using *rfp*-labeled pVSV208 in co-colonization experiments.

<u>Transcription of *hbtR* is activated as symbionts exit the light organ.</u> Considering the effects HbtR has on chemotaxis and luminescence gene expression (Tables 1 and S1), and that *hbtRC* has no effect on squid luminescence (Fig. S1) or colonization (Fig. 4C), we postulated that HbtR was likely to be involved in the transition into planktonic life as *V. fischeri* exits the light organ. To establish at which point in the juvenile squid diel cycle *V. fischeri hbtRC* expression is activated, we performed *in situ* hybridization chain reaction (HCR) targeting *hbtR* mRNA to determine whether this gene was expressed in the bacteria before, during, or after their expulsion from the squid light organ into seawater. *hbtR* mRNA was not detected in *V. fischeri* cells within the crypts or during expulsion along the path out of the light organ (Fig. 5A). Only in those cells that had completely exited the light organ pore was *hbtR* expression detected (Fig. 5B and Movie S1). Within an hour of expulsion into seawater, ~25% of expelled *V. fischeri* cells were expressing *hbtR* (Fig. 5C).

Discussion

While much research has gone into understanding the mechanisms necessary for colonization of the *E. scolopes* light organ by *V. fischeri* (reviewed most recently in (37)), there has been little investigation into how the ~95% of symbiotic bacteria expelled from the light organ at dawn each day transition back into life in seawater. In this work we present HbtR, a heterofunctional homolog of the *V. cholerae* virulence regulator TcpP that represses the quorum-signaling regulator LitR. Further, through the discovery of additional functions regulated by LitR, namely chemotaxis, motility, and EPS production, we have begun to build a picture in which LitR aids the transition by *V. fischeri* into a colonization lifestyle and, upon expulsion from the light organ, HbtR reverses that process to help transition back into planktonic life (Fig. 6). This is a markedly different role for HbtR from that of TcpP.

The regulatory mechanisms controlling *hbtRC* expression, as elucidated thus far, are similar to the *tcpPH* regulatory pathway in *V. cholerae* only in that both operons are regulated by the global regulator Crp, albeit in the opposite manner. Notably, the *hapR* homolog in *V. fischeri*, *litR*, is itself repressed by HbtR (Tables 1, S1), a reversal of roles from those in *V. cholerae*. Considering the distinct regulatory pathways for HbtR and TcpP and the low percent identity (26.8%) of the two protein sequences, it appears, evolutionarily, that either progenitors of *tcpPH* and *hbtRC* were acquired independently after separation of the two species' ancestors, or the parent operon evolved in dramatically different fashions as the two species evolved to inhabit disparate environmental niches. Determining which of these histories is the more likely is beyond

the scope of this study, but in either case it is clear the two homologs have been recruited into specialized roles befitting the two species' distinct lifestyles, i.e., pathogenesis versus beneficial symbiosis within animal hosts.

The data presented here are consistent with HbtR acting as a first-wave responder as *V. fischeri* bacteria exit the light organ and re-enter the seawater (Fig. 5), a significant change in environmental conditions and imperatives for survival. This role could explain some of the discrepancies observed between the RNA-seq results in the present study and those in Thompson 2017. For example, the Thompson data indicate that in addition to *hbtR* and *hbtC*, the luminescence genes *luxR*, *luxI*, and *luxCDABEG* were also highly upregulated in cells recently expelled from the light organs compared to planktonic cells, while *litR*, which activates the *lux* genes, was not differentially regulated between the two cell populations. Meanwhile, the results of this study indicate that HbtR represses LitR and consequently causes the downregulation of *lux* and other downstream quorum-signaling genes (Tables 1 and S1). Similarly, the gene most highly upregulated by HbtR in the RNA-seq data presented here was VF_2042 (Table S1), one of the four MCP genes repressed by LitR (Table 1); in the earlier study, VF_2042 was downregulated in cells released from the light organs (19). These results are consistent with a model in which HbtR becomes active once *V. fischeri* exits the light organ, with some of the earliest effects seen in its repression of *litR*. In the earlier study, it may have been that in the ~25 minutes between initiation of light-organ expulsion and harvesting the *V. fischeri* RNA, HbtR had become activated (Fig. 5) and was already repressing *litR* expression, but the downstream effects (e.g., on *lux* gene expression) were not yet apparent.

Previous studies have also demonstrated a repression of several flagellin genes by AinS and increased motility in a *litR* mutant (31). Here we show that LitR represses numerous flagellin, motor, and chemotaxis genes, including at least two MCP genes involved in chemotaxis toward $(GlcNAc)_2$, an *N*-acetylated sugar reported to be an important chemoattractant during light-organ colonization (12). Previous work indicated that a *litR* mutant colonized *E. scolopes* to a lower level than wild-type *V. fischeri* (31), which the authors suggested was due to an initiation delay due to hypermotility. However, in the study in which LitR was first described (4), a *litR* mutant had an advantage in initiating light-organ colonization over wild-type *V. fischeri.* Based on work presented here, including a demonstration that MCP genes repressed by LitR are involved in light-organ colonization (Fig. 2), we posit that the *litR*-mutant colonization benefit (4) may have been a priority effect (38), resulting from the increase in both motility and chemotaxis into the light organ by that mutant. We hypothesize that the lower level of colonization observed for the *litR* mutant in single-strain experiments (31) may have been due to dysregulation of a separate symbiotic process, perhaps extracellular polysaccharide production.

LitR appears to activate, and HbtR to thus repress, a large locus of genes (VF_0157–80) involved in extracellular polysaccharide production (Tables 1 and S1). Fidopiastis et al. (4) noted that *litR*$^-$ colonies are less opaque than wild-type *V. fischeri* and suggested this may be due to a difference in the extracellular polysaccharides present in each strain. The nature of polysaccharide affected by VF_0157–80 is not definite, yet it seems most likely to be EPS, or “slime layer,” due to the ease with which it separates from the bacterial cell during centrifugation (Fig. 3A). While

lipopolysaccharide and the *syp* polysaccharide have been implicated in the initiation of host colonization by *V. fischeri* (39–41), little has been determined regarding the possible involvement of extracellular polysaccharides in colonization persistence. *V. fischeri*-colonized crypts, despite having no goblet cells (Nyholm, personal communication), have been shown to stain alcian blue-positive (42), indicating the presumed EPS made by VF0157–80 may be a relevant factor in *E. scolopes*-*V. fischeri* symbiosis. This aspect of the symbiotic relationship could have broader implications for host-microbe interactions in general.

Materials and Methods

Bacterial strains and growth conditions. Bacterial strains and plasmids used in this study are summarized in Table S2. *E. coli* and *V. cholerae* were grown in lysogeny broth (LB; (43), (19)) at 37 °C; *V. fischeri* was grown in LB-salt (LBS; (44)) at 28 °C. Overnight cultures were inoculated with single colonies from freshly streaked -80 °C stocks. Liquid cultures were shaken at 225 rpm. Unless otherwise noted, 15 g of agar were added per liter for solid media. Antibiotics were added to overnight cultures, where applicable, at the following concentrations: kanamycin (Km), 50 µg/mL; chloramphenicol (Cm), 5 µg/mL (*V. fischeri*) or 25 µg/mL (*E. coli*). Experimental cultures were grown in either seawater-tryptone (SWT) medium (45) or minimal-salts medium (MSM; per L: 8.8 g NaCl, 6.2 g $MgSO_4 \cdot 7H_2O$, 0.74 g $CaCl_2 \cdot 2H_2O$, 0.0204 g H_2NaPO_4, 0.37 g KCl, 8.66 g PIPES disodium salt, 0.65 mg $FeSO_4 \cdot 7H_2O$; pH 7.5) supplemented with 0.005 g/L casamino acids and a carbon source as indicated. The results of all experiments are

reported as the means of three (or more, as indicated) biological replicates ± 1 standard deviation (SD). Statistical analysis was performed using Welch's t-test.

Plasmid and mutant construction. Primers used to construct the deletion and expression vectors in this study are listed in Table S3. In-frame deletion of genes from the *V. fischeri* genome was performed as previously described (46, 47). Counter-selection to remove the target gene and pSMV3 was performed on LB-sucrose (per L: 2.5 g NaCl, 10 g Bacto Tryptone, 5 g yeast extract, 100 g sucrose) for two days at room temperature. Expression vectors were constructed by amplifying and ligating the target gene into the multiple cloning site of pVSV105 (48). Inducible expression of *hbtRC* was achieved by ligating *lacI*^{q} from pAKD601 to *hbtRC* cloned from the *V. fischeri* genome and inserting the fusion into the multiple cloning site of pVSV105. Overexpression of *hbtRC* brought the level of expression closer to that found upon expulsion from juvenile squid (19), which was higher than we measured for wild-type *V. fischeri* in culture conditions. Genomic insertion of *gfp* or *rfp* under control of the *lac* promoter at the *attTn7* site was performed using a mini-Tn7 vector as described (49). Previously constructed Δ*hbtRC* (19) was used to recapitulate conditions for follow-up on previous experiments (RNA-seq and squid co-colonization); a newly derived Δ*hbtRC* strain was used for all other experiments so it would have the same parent wild-type *V. fischeri* stock as other mutants created in this study.

Generation and analysis of RNAseq libraries. RNA extraction and RNAseq were performed as previously described (19). Briefly, RNA was stabilized with RNAprotect Bacterial Reagent (Qiagen) and extracted with an RNeasy Mini Kit (Qiagen) from 500 µL of cultures grown to mid-log phase in SWT with 1.75 mM IPTG. RNA was extracted

from biological triplicates for each strain. Contaminating DNA was degraded by treatment with TURBO DNase (Invitrogen). Ribosomal reduction, strand-specific library preparation, and paired-end 50-bp sequence analysis on an Illumina HiSeq 2500 on high-output mode were performed at the University of Minnesota Genomics Center. Sequences were processed on the open-source Galaxy server (usegalaxy.org; (50)) using the following workflow (default settings used unless otherwise indicated): reads were trimmed with Trimmomatic (maximum mismatch:1, LEADING:3, TRAILING:3, SLIDINGWINDOW:4,20, MINLEN:35), mapped to the *V. fischeri* chromosomes and plasmid (accession nos. NC_006840.2, NC_006841.2, and NC_006842.2) using Bowtie2 (-un-con, --sensitive), and counted with featureCounts (-p disabled, -t=gene, -g=locus_tag, -Q=10, -s); differential expression was analyzed with DESeq2 (outliers filtering and independent filtering turned on). Between 11.7 million and 12.7 million paired reads were mapped to the *V. fischeri* genome per biological replicate.

Reverse transcription and quantitative PCR. RNA from bacterial cultures was extracted as described above and treated with TURBO DNase (Invitrogen). cDNA was synthesized from DNase-treated RNA using SMART MMLV Reverse Transcriptase (Clontech) and Random Hexamer Primer (Thermo Scientific). Gene expression was measured by qPCR performed with LightCycler 480 SYBR Green I Master Mix (Roche) under the following conditions: 95°C for 5 min; 45 cycles of 95°C for 10 sec, 60°C for 20 sec, and 72°C for 20 sec; melting curve acquisition from 65°C to 97°C. Cycle thresholds (Ct) for each sample were normalized to those of the reference gene *polA* (ΔCt = target gene-*polA*; *polA* expression primers provided courtesy Silvia Moriano-Gutierrez). ΔΔCt

values were calculated by subtracting the average ΔCt for the parent strain, at higher pH or lower OD_{600} when appropriate; fold changes were calculated as $2^{(-\Delta\Delta Ct)}$.

Growth and luminescence curves. Overnight LBS cultures of each strain were pelleted, washed once, and resuspended in 1 mL of the intended growth medium. Luminescence growth curves were performed in 20 mL SWT in flasks shaking at 225 rpm; periodic 1 mL and 300 µL aliquots were taken for luminescence and OD_{600} readings on a luminometer (Turner Designs) and Tecan Genios plate reader, respectively. Growth curves were performed in 1.2 mL growth medium and monitored in the Tecan Genios plate reader with continuous shaking at high speed.

Squid colonization assays. Juvenile squid colonization experiments were performed as described previously (38), with juvenile squid exposed to *V. fischeri* strains at 1,000–6,000 CFU/mL either for 3 h or overnight, as indicated, before being placed in fresh sterile seawater until euthanizing by freezing. Colonization competition experiments were performed by exposing juvenile squid to a 1:1 inoculum of each strain.

***In situ* hybridization chain reaction.** HCR (51) was performed on squid colonized with wild-type *V. fischeri* carrying a *gfp*-labeled plasmid and on *V. fischeri* cells 1 h after being expelled from squid light organs as previously described (52–54). Briefly, *E. scolopes* juveniles and expelled *V. fischeri* cells were fixed in 4% paraformaldehyde in marine phosphate-buffered saline either before or after a light cue stimulated bacterial expulsion. HCR was performed on dissected light organs (52) and expelled *V. fischeri* cells affixed to gelatin-coated slides (adapted from (53)) but using HCR version 3.0 chemistry (54). Ten probes targeting *hbtR* mRNA (Table 2) were amplified with Alexa Fluor 546-labeled hairpins (Molecular Instruments). Light organs were then

counterstained overnight with a 1:750 dilution of 4′,6-diamidino-2-phenylindole (DAPI; Thermo Fisher Scientific) in 5x SSC-Tween before mounting on slides with Vectashield (Vector Laboratories) and overlaid with a coverslip (#1.5, Fisherbrand, Fisher Scientific). All imaging was done on an upright Zeiss LSM 710 laser-scanning confocal microscope at the University of Hawai‘i Kewalo Marine Laboratory and images were analyzed using FIJI (ImageJ) (55).

Motility and chemotaxis assays. Soft-agar motility assays were performed as previously described (56). Briefly, the equivalent of 10 µL bacteria grown to an OD_{600} of 0.5 in SWT were spotted onto minimal-medium plates containing 0.25% agar and, when appropriate, 1 mM chemoattractant. Migration zones were measured after 18–24 h of static incubation at 28°C.

Alcian blue detection of extracellular polysaccharides. EPS was detected by staining with alcian blue essentially as previously described (57). Single colonies from freshly streaked -80°C stocks were used to inoculate MSM supplemented with 6.5 mM Neu5Ac and 0.05% casamino acids and grown with shaking 18–22 h. EPS was separated from cells by centrifugation of the equivalent of 2.5 mL at OD_{600}=1.0 for 15 min at 12,000 xg and 4°C. 250 µL of this supernatant was mixed with 1 mL alcian-blue solution (per L: 0.5 g alcian blue, 30 mL glacial acetic acid, pH 2.5) for 1 h at room temperature, then centrifuged for 10 min at 10,000 rpm and 4°C. Pellets were resuspended in 1 mL 100% ethanol, then centrifuged for 10 min at 10,000 xg and 4°C. Pellets were solubilized in 500 µL SDS (per L: 100 g sodium dodecyl sulfate, 50 mM sodium acetate, pH 5.8), and the absorbance was read at OD_{620}.

Acknowledgments

The authors thank Silvia Moriano-Gutierrez and Alexandrea Duscher for advice regarding RNA-seq, Elliott McCloskey and Roxane Gaedeke for help with experiment execution, the University of Minnesota Genomics Center for RNA processing and next-generation sequencing, and the Ruby and McFall-Ngai laboratories for their insights. The research was supported by NIH grants R37 AI50661 (Margaret McFall-Ngai and E.G.R.), R01 OD11024, and GM135254 (E.G.R. and M.M.-N.) and NSF INSPIRE Grant MCB1608744 (Eva Kanso and Scott Fraser). Acquisition of the Leica TCS SP8 X confocal was supported by NSF DBI 1828262 (Marilyn Dunlap, E.G.R., and M.M.-N.), and microscopy was performed in the MICRO facility, supported by COBRE P20 GM125508 (M.M.-N. and E.G.R.).

References

1. Eberhard A, Burlingame AL, Eberhard C, Kenyon GL, Nealson KH, Oppenheimer NJ. 1981. Structural identification of autoinducer of *Photobacterium fischeri* luciferase. Biochemistry 20:2444–2449.
2. Kuo A, Blough NV, Dunlap PV. 1994. Multiple N-acyl-L-homoserine lactone autoinducers of luminescence in the marine symbiotic bacterium *Vibrio fischeri*. J Bacteriol 176:7558–7565.
3. Eberhard A. 1972. Inhibition and activation of bacterial luciferase synthesis. J Bacteriol 109:1101–1105.
4. Fidopiastis PM, Miyamoto CM, Jobling MG, Meighen EA, Ruby EG. 2002. LitR, a new transcriptional activator in *Vibrio fischeri*, regulates luminescence and symbiotic light organ colonization. Mol Microbiol 45:131–143.
5. Engebrecht J, Silverman M. 1984. Identification of genes and gene products necessary for bacterial bioluminescence. Proc Natl Acad Sci U S A 81:4154–4158.
6. Verma SC, Miyashiro T. 2013. Quorum sensing in the squid-*Vibrio* symbiosis. Int J Mol Sci 14:16386–16401.

7. Visick KL, Foster J, Doino J, McFall-Ngai M, Ruby EG. 2000. *Vibrio fischeri lux* genes play an important role in colonization and development of the host light organ. J Bacteriol 182:4578–4586.
8. Koch EJ, Miyashiro T, McFall-Ngai MJ, Ruby EG. 2014. Features governing symbiont persistence in the squid-vibrio association. Mol Ecol 23:1624–1634.
9. Moriano-Gutierrez S, Koch EJ, Bussan H, Romano K, Belcaid M, Rey FE, Ruby EG, McFall-Ngai MJ. 2019. Critical symbiont signals drive both local and systemic changes in diel and developmental host gene expression. Proc Natl Acad Sci U S A 116:7990-7999.
10. Wei SL, Young RE. 1989. Development of symbiotic bacterial bioluminescence in a nearshore cephalopod, *Euprymna scolopes*. Marine Biol 103:541–546.
11. Graf J, Dunlap PV, Ruby EG. 1994. Effect of transposon-induced motility mutations on colonization of the host light organ by *Vibrio fischeri*. J Bacteriol 176:6986–6991.
12. Mandel MJ, Schaefer AL, Brennan CA, Heath-Heckman EA, Deloney-Marino CR, McFall-Ngai MJ, Ruby EG. 2012. Squid-derived chitin oligosaccharides are a chemotactic signal during colonization by *Vibrio fischeri*. Appl Environ Microbiol 78:4620–4626.
13. Ruby EG, Asato LM. 1993. Growth and flagellation of Vibrio fischeri during initiation of the sepiolid squid light organ symbiosis. Arch Microbiol 159:160–167.
14. Graf J, Ruby EG. 1998. Host-derived amino acids support the proliferation of symbiotic bacteria. Proc Natl Acad Sci U S A 95:1818–1822.
15. Jones BW, Nishiguchi MK. 2004. Counterillumination in the Hawaiian bobtail squid, *Euprymna scolopes* Berry (Mollusca: Cephalopoda). Mar Biol 144:1151–1155.
16. Stabb EV, Millikan DS. 2009. Is the *Vibrio fischeri-Euprymna scolopes* symbiosis a defensive mutualism? p. 85–98. *In*: White JF Jr., Torres MS (ed.), Defensive Mutualism in Microbial Symbiosis. CRC Press, Boca Raton, FL.
17. Lee K H, Ruby E G. 1994. Effect of the squid host on the abundance and distribution of symbiotic *Vibrio fischeri* in nature. Appl Environ Microbiol 60:1565–1571.
18. Nyholm SV, McFall-Ngai MJ. 1998. Sampling the light-organ microenvironment of *Euprymna scolopes*: description of a population of host cells in association with the bacterial symbiont *Vibrio fischeri*. Biol Bull 195:89–97.
19. Thompson LR, Nikolakakis K, Pan S, Reed J, Knight R, Ruby EG. 2017. Transcriptional characterization of *Vibrio fischeri* during colonization of juvenile *Euprymna scolopes*. Environ Microbiol 19:1845–1856.
20. Thomas S, Williams SG, Manning PA. 1995. Regulation of *tcp* genes in classical and El Tor strains of *Vibrio cholerae* O1. Gene 166:43–48.
21. Häse CC, Mekalanos JJ. 1998. TcpP protein is a positive regulator of virulence gene expression in *Vibrio cholerae*. Proc Natl Acad Sci U S A 95:730–734.

22. Taylor R K, Miller V L, Furlong D B, Mekalanos J J. 1987. Use of *phoA* gene fusions to identify a pilus colonization factor coordinately regulated with cholera toxin. Proc Natl Acad Sci U S A 84:2833–2837.

23. Skorupski K, Taylor RK. 1999. A new level in the *Vibrio cholerae* ToxR virulence cascade: AphA is required for transcriptional activation of the *tcpPH* operon. Mol. Microbiol 31:763–771.

24. Kovacikova G, Skorupski K. 1999. A *Vibrio cholerae* LysR homolog, AphB, cooperates with AphA at the *tcpPH* promoter to activate expression of the ToxR virulence cascade. J Bacteriol 181:4250–4256.

25. Kovacikova G, Lin W, Skorupski K. 2010. The LysR-type virulence activator AphB regulates the expression of genes in *Vibrio cholerae* in response to low pH and anaerobiosis. J Bacteriol 192:4181–4191.

26. Zhu J, Miller MB, Vance RE, Dziejman M, Bassler BL, Mekalanos JJ. 2002. Quorum-sensing regulators control virulence gene expression in *Vibrio cholerae*. Proc Natl Acad Sci U S A 99:3129–3134.

27. Kovacikova G, Skorupski K. 2002. Regulation of virulence gene expression in *Vibrio cholerae* by quorum sensing: HapR functions at the *aphA* promoter. Mol Microbiol 46:1135–1147.

28. Kovacikova G, Skorupski K. 2001. Overlapping binding sites for the virulence gene regulators AphA, AphB and cAMP-CRP at the *Vibrio cholerae tcpPH* promoter. Mol Microbiol 41:393–407.

29. Larocque RC, Harris JB, Dziejman M, Li X, Khan AI, Faruque AS, Faruque SM, Nair GB, Ryan ET, Qadri F, Mekalanos JJ, Calderwood SB. 2005. Transcriptional profiling of *Vibrio cholerae* recovered directly from patient specimens during early and late stages of human infection. Infect Immun 73:4488–4493.

30. Schild S, Tamayo R, Nelson EJ, Qadri F, Calderwood SB, Camilli A. 2007. Genes induced late in infection increase fitness of *Vibrio cholerae* after release into the environment. Cell Host Microbe 2:264–277.

31. Lupp C, Ruby EG. 2005. *Vibrio fischeri* uses two quorum-sensing systems for the regulation of early and late colonization factors. J Bacteriol 187:3620–3629.

32. Cao X, Studer SV, Wassarman K, Zhang Y, Ruby EG, Miyashiro T. 2012. The novel sigma factor-like regulator RpoQ controls luminescence, chitinase activity, and motility in *Vibrio fischeri*. mBio pii:e00285-11.

33. Dunlap PV, Greenberg EP. 1985. Control of *Vibrio fischeri* luminescence gene expression in *Escherichia coli* by cyclic AMP and cyclic AMP receptor protein. J Bacteriol 164:45–50.

34. Lyell NL, Colton DM, Bose JL, Tumen-Velasquez MP, Kimbrough JH, Stabb EV. 2013. Cyclic AMP receptor protein regulates pheromone-mediated bioluminescence at multiple levels in *Vibrio fischeri* ES114. J Bacteriol 195:5051–5063.

35. Murley YM, Carroll PA, Skorupski K, Taylor RK, Calderwood SB. 1999. Differential transcription of the *tcpPH* operon confers biotype-specific control of the *Vibrio cholerae* ToxR virulence regulon. Infect Immun 67:5117–23.

36. Krukonis ES, Yu RR, DiRita VJ. 2000. The *Vibrio cholerae* ToxR/TcpP/ToxT virulence cascade: distinct roles for two membrane-localized transcriptional activators on a single promoter. Mol Microbiol 38:67–84.

37. Norsworthy AN, Visick KL. 2013. Gimme shelter: how *Vibrio fischeri* successfully navigates an animal's multiple environments. Front Microbiol 4:356.

38. Bongrand C, Ruby EG. 2019. Achieving a multi-strain symbiosis: strain behavior and infection dynamics. ISME J 13:698–706.

39. Yip ES, Grublesky BT, Hussa EA, Visick KL. 2005. A novel, conserved cluster of genes promotes symbiotic colonization and sigma-dependent biofilm formation by *Vibrio fischeri*. Mol Microbiol 57:1485–1498.

40. Post DM, Yu L, Krasity BC, Choudhury B, Mandel MJ, Brennan CA, Ruby EG, McFall-Ngai MJ, Gibson BW, Apicella MA. 2012. O-antigen and core carbohydrate of *Vibrio fischeri* lipopolysaccharide: composition and analysis of their role in *Euprymna scolopes* light organ colonization. J Biol Chem 287:8515–8530.

41. Schwartzman JA, Lynch JB, Flores Ramos S, Zhou L, Apicella MA, Yew JY, Ruby EG. 2019. Acidic pH promotes lipopolysaccharide modification and alters colonization in a bacteria-animal mutualism. Mol Microbiol 112:1326–1338.

42. Nyholm SV, Deplancke B, Gaskins HR, Apicella MA, McFall-Ngai MJ. 2002. Roles of *Vibrio fischeri* and nonsymbiotic bacteria in the dynamics of mucus secretion during symbiont colonization of the *Euprymna scolopes* light organ. Appl Environ Microbiol 68:5113–5122.

43. Bertani G. 1951. Studies on lysogenesis. I: The mode of phage liberation by lysogenic *Escherichia coli*. J Bacteriol 62:293–300.

44. Stabb EV, Reich KA, Ruby EG. 2001. *Vibrio fischeri* genes *hvnA* and *hvnB* encode secreted NAD(+)-glycohydrolases. J Bacteriol 183:309–317.

45. Boettcher KJ, Ruby EG. 1990. Depressed light emission by symbiotic *Vibrio fischeri* of the sepiolid squid *Euprymna scolopes*. J Bacteriol 172:3701–3706.

46. Saltikov CW, Newman DK. 2003. Genetic identification of a respiratory arsenate reductase. Proc Natl Acad Sci U S A 100:10983–10988.

47. Bennett BD, Redford KE, Gralnick JA. 2018. Survival of anaerobic Fe^{2+} stress requires the ClpXP protease. J Bacteriol 200. pii:e00671-17.

48. Dunn AK, Millikan DS, Adin DM, Bose JL, Stabb EV. 2006. New *rfp*- and pES213-derived tools for analyzing symbiotic *Vibrio fischeri* reveal patterns of infection and *lux* expression in situ. Appl Environ Microbiol 2:802–810.

49. McCann J, Stabb EV, Millikan DS, Ruby EG. 2003. Population dynamics of *Vibrio fischeri* during infection of Euprymna scolopes. Appl Environ Microbiol 69:5928–5934.

50. Afgan E, Baker D, Batut B, van den Beek M, Bouvier D, Cech M, Chilton J, Clements D, Coraor N, Grüning BA, Guerler A, Hillman-Jackson J, Hiltemann S, Jalili V, Rasche H, Soranzo N, Goecks J, Taylor J, Nekrutenko A, Blankenberg D. 2018. The Galaxy platform for accessible, reproducible and collaborative biomedical analyses: 2018 update. Nucleic Acids Res 46:W537–W544.

51. Choi HM, Chang JY, Trinh le A, Padilla JE, Fraser SE, Pierce NA. 2010. Programmable in situ amplification for multiplexed imaging of mRNA expression. Nat Biotechnol 28:1208–1212.

52. Nikolakakis K, Lehnert E, McFall-Ngai MJ, Ruby EG. 2015. Use of Hybridization Chain Reaction-Fluorescent In situ hybridization to track gene expression by both partners during initiation of symbiosis. Appl Environ Microbiol 81:4728–4735.

53. Choi HM, Calvert CR, Husain N, Huss D, Barsi JC, Deverman BE, Hunter RC, Kato M, Lee SM, Abelin AC, Rosenthal AZ, Akbari OS, Li Y, Hay BA, Sternberg PW, Patterson PH, Davidson EH, Mazmanian SK, Prober DA, van de Rijn M, Leadbetter JR, Newman DK, Readhead C, Bronner ME, Wold B, Lansford R, Sauka-Spengler T, Fraser SE, Pierce NA. 2016. Mapping a multiplexed zoo of mRNA expression. Development 143:3632–3637.

54. Choi HMT, Schwarzkopf M, Fornace ME, Acharya A, Artavanis G, Stegmaier J, Cunha A, Pierce NA. 2018. Third-generation in situ hybridization chain reaction: multiplexed, quantitative, sensitive, versatile, robust. Development 145:dev165753.

55. Schindelin J, Arganda-Carreras I, Frise E, Kaynig V, Longair M, Pietzsch T, Preibisch S, Rueden C, Saalfeld S, Schmid B, Tinevez JY, White DJ, Hartenstein V, Eliceiri K, Tomancak P, Cardona A. 2012. Fiji: An open-source platform for biological-image analysis. Nat Methods 9:676–682.

56. DeLoney-Marino CR. 2013. Observing chemotaxis in *Vibrio fischeri* using soft agar assays in an undergraduate microbiology laboratory. J Microbiol Biol Educ 14:271–272.

57. Plante CJ. 2000. Role of bacterial exopolymeric capsules in protection from deposit-feeder digestion. Aquat Microb Ecol 21:211–219.

58. Bongrand C, Koch EJ, Moriano-Gutierrez S, Cordero OX, McFall-Ngai M, Polz MF, Ruby EG. 2016. A genomic comparison of 13 symbiotic *Vibrio fischeri* isolates from the perspective of their host source and colonization behavior. ISME J 10:2907–2917.

59. Mekalanos JJ, Swartz DJ, Pearson GD, Harford N, Groyne F, de Wilde M. 1983. Cholera toxin genes: nucleotide sequence, deletion analysis and vaccine development. Nature 306:551–557.

60. Liss L. 1987. New M13 host: DH5 F’ competent cells. Focus 9:13.

61. Bao Y, Lies DP, Fu H, Roberts GP. 1991. An improved Tn7-based system for the single-copy insertion of cloned genes into chromosomes of gram-negative bacteria. Gene 109:167–168.

62. Stabb EV, Ruby EG. 2002. RP4-based plasmids for conjugation between *Escherichia coli* and members of the vibrionaceae. Method Enzymol 358:413–426.

63. Coursolle D, Gralnick JA. 2010. Modularity of the Mtr respiratory pathway of *Shewanella oneidensis* strain MR-1. Mol Microbiol 77:995–1008.

641

Table 1. RT-qPCR results[a]

	Wild-type *V. fischeri*		Δ*litR*			
Gene	**ΔCt[b] (gene-*polA*)**	**SD**	**ΔCt (gene-*polA*)**	**SD**	***p*-value[c]**	**Fold change**
VF1133	3.01	0.03	1.12	0.07	0.001	3.70
VF2042	4.64	0.15	-1.73	0.52	0.002	86.13
VFA0246	3.87	0.06	-1.47	0.12	0.000	40.32
VFA0389	0.52	0.15	-0.81	0.18	0.002	2.52
cheW	-1.55	0.05	-2.53	0.24	0.019	1.99
motA1	0.95	0.23	-0.16	0.30	0.015	2.17
flaC	-1.58	0.22	-4.17	0.51	0.015	6.27
flaF	1.31	0.14	-1.44	0.75	0.024	7.41
rpoN	-0.01	0.14	0.14	0.11	0.233	0.90
flrA	-0.74	0.04	-0.48	0.12	0.071	0.84
flrB	0.85	0.13	1.38	0.63	0.293	0.74
fliA	-1.37	0.11	-1.81	0.27	0.119	1.38
flgM	-0.53	0.14	-1.35	0.31	0.053	1.80
wbfB	1.56	0.12	3.72	0.24	0.005	0.23
etp	0.38	0.09	3.42	0.08	< 0.0001	0.12
wzc	0.35	0.20	3.46	0.17	0.000	0.12

	Low Cell Density				High Cell Density			
Strain	**ΔCt (*hbtRC-polA*)**	**SD**	***p*-value**	**Fold change**	**ΔCt (*hbtRC-polA*)**	**SD**	***p*-value[d]**	**Fold change**
Wild-type *V. fischeri*	8.08	0.12	—	—	13.07	0.35	0.002	0.03
Δ*litR*	8.19	0.58	0.775	0.97	13.02	0.69	0.007	0.04
Δ*crp*	10.06	0.68	0.038	0.27	12.29	0.12	< 0.0001	0.05

	Low Cell Density				High Cell Density			
Condition	**ΔCt (*hbtRC-polA*)**	**SD**	***p*-value**	**Fold change**	**ΔCt (*hbtRC-polA*)**	**SD**	***p*-value[e]**	**Fold change**
SWT Alone	6.00	0.49	—	—	10.04	0.53	0.002	0.06
+ C8-HSL	5.72	0.13	0.473	1.25	10.60	0.87	0.001	0.06
+ 3-oxo-C6-HSL	5.71	0.39	0.432	1.22	10.16	0.26	0.004	0.05

	Wild-type *V. fischeri*				Δ*aphB*			
pH[f]	**ΔCt (*hbtRC-polA*)**	**SD**	***p*-value**	**Fold change**	**ΔCt (*hbtRC-polA*)**	**SD**	***p*-value[g]**	**Fold change**
8.5	10.94	0.37	—	—	10.42	0.33	0.167	1.46
5.5	10.55	0.14	0.227	1.32	10.34	0.34	0.132	1.54

Strain	ΔCt (*litR-polA*)	SD	*p*-value	Fold change
Δ*hbtRC* + empty vector	-4.38	0.19	—	—
Δ*hbtRC* + *hbtRC*	-3.46	0.42	0.032	0.54
Δ*hbtRC* + *tcpPH*	-4.65	0.05	0.131	1.20

Strain[h]	ΔCt (*toxT-polA*)	SD	*p*-value	Fold change
Δ*tcpPH* + empty vector	4.90	0.40	—	—
Δ*tcpPH* + *tcpPH*	-0.06	0.28	0.0004	31.65
Δ*tcpPH* + *hbtRC*	4.61	0.52	0.498	1.27

Strain	ΔCt (*litR-polA*)	SD	*p*-value	Fold change
Δ*hbtRC* + empty vector	-2.19	0.17	—	—
Δ*hbtRC* + *hbtRC*	-0.29	0.32	0.003	0.27
Δ*hbtRC*Δ*toxRS* + empty vector	-1.57	0.96	0.188	1.19
Δ*hbtRC*Δ*toxRS* + *hbtRC*	-0.72	0.26	0.004	0.37

[a] All cultures grown in SWT unless otherwise noted
[b] ΔCt, avg of three biological replicates
[c] *p*-value determined from ΔCt values using Welch's t-test
[d] *p*>0.05 for Δ*litR* and Δ*crp* at high density vs. wild-type at high density
[e] *p*>0.05 for + C8-HSL and + 3-oxo-C6 at high density vs. SWT alone at high density
[f] Cultures grown in MSM buffered to indicated pH and supplemented with 7.5 mM GlcNAc and 0.05% casamino acids
[g] *p*>0.05 for Δ*aphB* vs. wild-type at pH 5.5
[h] Cultures grown in LB

Table 2. Soft-agar migration zone sizes

	GlcNAc			$(GlcNAc)_2$			Neu5Ac		
Strain	**Zone size (mm)[a]**	**SD[b]**	***p*-value[c]**	**Zone size (mm)**	**SD**	***p*-value**	**Zone size (mm)**	**SD**	***p*-value**
Wild-type *V. fischeri*	25.7	0.6	—	21.7	0.6	—	24	1	—
ΔVF_1133	18.0	0.0	< 0.0001	14.0	0.0	< 0.0001	18	1	0.002
ΔVF_2042	26.3	0.6	0.230	21.3	0.6	0.519	25	1.7	0.450
ΔVF_A0246	19.7	0.6	0.0002	16.3	0.6	0.0003	19.7	0.6	0.007
ΔVF_A0389	26.0	1.0	0.651	22.0	1.7	0.782	24	0	0.651
ΔVF_1133 ΔVF_A0246	ND	ND	ND	ND	ND	ND	17.7	0.6	0.003
ΔΔΔΔ	19.3	2.1	0.037	15.3	1.2	0.014	23.7	3.2	0.880

	Glucose			No chemoattractant		
Strain	**Zone size (mm)**	**SD**	***p*-value**	**Zone size (mm)**	**SD**	***p*-value**
Wild-type *V. fischeri*	18.2	0.8	—	17.0	0.0	—
ΔΔΔΔ	19.2	2.9	0.455	16.7	0.6	0.230

	GlcNAc			No chemoattractant		
Strain	**Zone size (mm)**	**SD**	***p*-value**	**Zone size (mm)**	**SD**	***p*-value**
Wild-type *V. fischeri* + empty vector	10.3	1.2	—	6.0	1.0	—
Wild-type *V. fischeri* + *hbtRC*	13.7	1.2	0.024	9.0	1.0	0.021
Wild-type *V. fischeri* + *litR*	5.3	0.6	0.022	5.3	0.6	0.391
Δ*litR* + empty vector	18.7	0.6	0.008	17.7	1.5	0.002
Δ*litR* + *hbtRC*	20.7	0.6	0.005	18.3	1.2	0.001
Δ*litR* + *litR*	6.0	1.0	0.016	7.7	0.6	0.088
Δ*rpoQ* + empty vector	10.7	0.6	0.699	5.0	0.0	0.139
Δ*rpoQ* + *hbtRC*	15.3	1.2	0.006	9.7	1.5	0.040
Δ*rpoQ* + *litR*	4.7	0.6	0.017	5.3	0.6	0.391

[a] Zone sizes are averages of at least three biological replicates
[b] *p*-value, Welch's t-test as compared to wild-type zones in that chemoattractant
[c] ND, not done

Table S2. Bacterial strains and plasmids used in this work.

Strain	Description	Source
ES114	*Vibrio fischeri*, wild-type	(45)
BDB127	ES114 with empty pVSV105	This work
BDB128	ES114 with pVSV105::*hbtRC*	This work
BDB171	ES114 with pVSV105::*litR*	This work
BDB156	ES114 with pVSV102	(48)
BDB011	ES114 with pVSV208	(48)
CBNR46	ES114 *att*Tn*7*:: P_{lac}-*gfp-erm*	(58)
CBNR47	ES114 *att*Tn*7*:: P_{lac}-*rfp-erm*	(58)
BDB003	ES114 Δ*hbtRC* (VF_A0473–A0474)	(19)
BDB134	ES114 Δ*hbtRC* (VF_A0473–A0474), newly derived	This work
BDB023	Δ*hbtRC* (BDB003) with pVSV105::*lacI-hbtRC*	This work
BDB039	Δ*hbtRC* (BDB003) with empty pVSV105	This work
BDB139	Δ*hbtRC* (BDB134) with empty pVSV105	This work
BDB140	Δ*hbtRC* (BDB134) with pVSV105::*hbtRC*	This work
BDB154	Δ*hbtRC* (BDB134) with pVSV105::*tcpPH*	This work
BDB157	Δ*hbtRC* (BDB134) with pVSV102	This work

BDB012	Δ*hbtRC* (BDB134) with pVSV208	This work
BDB078	Δ*hbtRC* (BDB003) *att*Tn*7*:: P_{lac}-*gfp-erm*	This work
BDB079	Δ*hbtRC* (BDB003) *att*Tn*7*:: P_{lac}-*rfp-erm*	This work
BDB172	Δ*hbtRC* Δ*toxRS* (VF_0790–91)	This work
BDB173	Δ*hbtRC* Δ*toxRS* with empty pVSV105	This work
BDB174	Δ*hbtRC* Δ*toxRS* with pVSV105::*hbtRC*	This work
BDB182	ES114 Δ*litR* (VF_2177)	This work
BDB183	Δ*litR* with empty pVSV105	This work
BDB184	Δ*litR* with pVSV105::*hbtRC*	This work
BDB185	Δ*litR* with pVSV105::*litR*	This work
BDB129	ES114 ΔVF0157–80	This work
BDB186	ΔVF0157–80 with empty pVSV105	This work
BDB187	ΔVF0157–80 with pVSV105::*hbtRC*	This work
BDB188	ΔVF0157–80 with pVSV105::*litR*	This work
BDB135	ES114 ΔVF_2042	This work
BDB141	ES114 ΔVF_1133	This work
BDB142	ES114 ΔVF_A0389	This work
BDB144	ES114 ΔVF_A0246	This work

BDB163	ES114 ΔVF_1133 ΔVF_2042 ΔVF_A0246 ΔVF_A0389	This work
CA1	Δ*rpoQ* (VF_A1015)	(32)
BDB194	Δ*rpoQ* with empty pVSV105	This work
BDB195	Δ*rpoQ* with pVSV105::*hbtRC*	This work
BDB176	Δ*rpoQ* with pVSV105::*litR*	This work
0395-N1	*V. cholerae* Ogawa 395 Δ*ctxA*	(59)
BDB190	0395-N1 Δ*tcpPH* (ΔVC0395_A0351-A0352)	This work
BDB191	Δ*tcpPH* with empty pVSV105	This work
BDB192	Δ*tcpPH* with pVSV105::*hbtRC*	This work
BDB193	Δ*tcpPH* with pVSV105::*tcpPH*	This work
DH5α*pir*	*E. coli* cloning strain; *recA1 endA1 hsdR17 supE44 thi-1 Δ(lacZYA-argF)U169 [Φ80dlacZΔM15] gyrA96 relA1 λpir+*	(60)
WM3064	*E. coli* conjugation strain; *thrB1004 pro thi rpsL hsdS lacZΔM15 RP4-1360 Δ(araBAD)567 ΔdapA1341::[erm pir(wt)]*	(46)

Plasmid	Description	Source
pAKD601	IPTG-inducible expression vector	(48)
pVSV105	Cloning vector; Cm^r	(48)
pVSV105::*lacI-hbtRC*	*lacI*^{q}-*A1*/*O4*/*O3*p from pAKD601, 26 bp upstream of *lacI*^{q}, 7 bp downstream of *A1*/*O4*/*O3*p; *hbtRC*, 18 bp upstream, 48 bp downstream; Cm^r	This work
pVSV105::*hbtRC*	*hbtRC*, 18 bp upstream, 48 bp downstream; Cm^r	This work
pVSV105::*litR*	*litR*, 21 bp upstream, 87 bp downstream; Cm^r	This work
pVSV105::*tcpPH*	*tcpPH*, 20 bp upstream, 2 bp downstream; Cm^r	This work
pVSV102	*gfp*; Km^r	(48)
pVSV208	*rfp*; Cm^r	(48)
pEVS107	mini-Tn7 vector; Km^r, Em^r	(49)
pCBNR6	pEVS107::P_{lac}-*gfp*; Km^r, Em^r	(58)
pCBNR7	pEVS107::P_{lac}-*rfp*; Km^r, Em^r	(58)
pUX-BF13	*tnsABCDE* transposase vector	(61)
pEVS104	Conjugation helper; Km^r	(62)

pSMV3	Deletion vector, Km^r, *sacB*	(63)
pSMV3Δ*hbtRC*	pSMV3 with VF_A0473–A0474 flanking sequences	This work
pSMV3Δ*litR*	pSMV3 with VF_2177 flanking sequences	This work
pSMV3ΔVF_0157-80	pSMV3 with VF_0157-80 flanking sequences	This work
pSMV3ΔVF_1133	pSMV3 with VF_1133 flanking sequences	This work
pSMV3ΔVF_2042	pSMV3 with VF_2042 flanking sequences	This work
pSMV3ΔVF_A0246	pSMV3 with VF_A0246 flanking sequences	This work
pSMV3ΔVF_A0389	pSMV3 with VF_A0389 flanking sequences	This work
pSMV3 ΔVC0395_ A0351-A0352	pSMV3 with VC0395_A0351-A0352 flanking sequences	This work

Table S3. Primers used in this work

Primer	Sequence	Restriction Site
lacI and *hbtRC* insertion into pVSV105		
lacIF2	CTAGGTCGACGCTAACTTACATTAATTGCGTTG	*Sal*I
lacIR	CTAGGAATTCCTGTGTGAAATTGTTATCCGC	*Eco*RI
hbtRF	CTAGGAATTCCTGTTAAGTCAGGATGATATGG	*Eco*RI
hbtCR	CATGGGTACCGTACCCTAAACACACTCTATAAATAAC	*Kpn*I
hbtRC insertion into pVSV105		
hbtRF2	CTAGTCTAGACTGTTAAGTCAGGATGATATGG	*Xba*I
hbtCR	CATGGGTACCGTACCCTAAACACACTCTATAAATAAC	*Kpn*I
litR insertion into pVSV105		
litRF	GTACGTCGACGTTGGCAAGGATATAAATATAATGG	*Sal*I
litRR	GTACGGTACCTTCTGATTAACAACGCATTTG	*Kpn*I
tcpPH insertion into pVSV105		
VCtcpPF	CATGTCTAGAGATTAAGAAAATGTAAAGTAATGG	*Xba*I
VCtcpHR	CATGGGTACCCCCTAAAAATCGCTTTGACAG	*Kpn*I
Gene deletion		
hbtRUSF	GATCGGATCCGAGAGCATTAAGTAGTGTTAATC	*Bam*Hi
hbtRUSR	GATCGGTACCCCATATCATCCTGACTTAACAG	*KpnI*
hbtCDSF	GATCGGTACCCAGCAGGAAGTGGTAGTCTC	*Kpn*I
hbtCDSR	GATCGAGCTCCAGGACTATTCGGGTTAAG	*Sac*I
litRUSF	GATCGGATCCGCATGATTAAGCGTTAAGATTAG	*Bam*HI
litRUSR	GATCGAATTCCCATTATATTTATATCCTTGCCAAC	*Eco*RI

774	litRDSF	GATCGAATTCCAAATTGTTTCTTAAATATGTTGTG	*Eco*RI
775	litRDSR	GATCGAGCTCGGTGGTATCATCGGTCTTG	*Sac*I
776	VF1133USF	GTACGGATCCGGTCACTTTGCACTCTCAC	*Bam*HI
777	VF1133USR	GTACGGTACCCTGTTCATGTTGTATCTCTCTTTC	*Kpn*I
778	VF1133DSF	GTACGGTACCGTAATTATCTTAGATAAGCAATGTC	*Kpn*I
779	VF1133DSR	GTACGAGCTCGCGTTTGGCATTGAGAATTG	*Sac*I
780	VF2042USF	GTACGAATTCGAAACCGTTTCAATCAAAACAG	*Eco*RI
781	VF2042USR	GTACGGTACCCATAGCTGCATACCTTAGTTATAAC	*Kpn*I
782	VF2042DSF	GTACGGTACCCTGTAATTAAGTTGATTTTTCACTTATG	*Kpn*I
783	VF2042DSR	GTACCTCGAGCCAGCTTTAATTGAGCCTTC	*Xho*I
784	VFA0246USF	GTACGGATCCCGCCTAATGCCTTCAATCG	*Bam*HI
785	VFA0246USR	GTACGGTACCCATAGATAACACCGCTGTAAG	*Kpn*I
786	VFA0246DSF	GTACGGTACCGTATAAAGGGTAATTCAATAGGCTG	*Kpn*I
787	VFA0246DSR	GTACGAGCTCCCAAGCCATCTCAATTTTACG	*Sac*I
788	VFA0389USF	GTACGGATCCGCCAGCCTTATCAGTTTTATTG	*Bam*HI
789	VFA0389USR	GTACGAATTCCTTCATAGAAACATCCTAAATCCG	*Eco*RI
790	VFA0389DSF	GTACGAATTCGTGTAACTGACGTATAACTATC	*Eco*RI
791	VFA0389DSR	GTACGAGCTCGCGTTACGACTATTGGTTTAC	*Sac*I
792	VF0157USF	GTACGGATCCGTCTAAAAATAAGAAAGCAGTGC	*Bam*HI
793	VF0157USR	GTACGGTACCGAAAAGGGCTTTGAGGGG	*Kpn*I
794	VF0180DSF	GTACGGTACCGATAAGCAAATAATGGCGTTTTG	*Kpn*I
795	VF0180DSR	GTACGAGCTCGAGTAACTTCGCTTAATGCC	*Sac*I
796	VF1690USF	GTACGGATCCCTGATCAATAAACAAGAGATAACG	*Bam*HI

797	VF1690USR	GTACGGTACCCTAATTTCATTATATTAAGATACTCTCC	*Kpn*I
798	VF1690DSF	GTACGGTACCGTAACCACATACCTGATTAATTTAC	*Kpn*I
799	VF1690DSR	GTACgagctcGTTTAGGTAAGCGTGAAATTG	*Sac*I
800	toxRUSF	GATCGGATCCGAACTCTTGGTATTCAGCATC	*Bam*HI
801	toxRUSR	GATCGGTACCCATCGGTTATTAACTCAGTAGTG	*Kpn*I
802	toxSDSF	GATCGGTACCCTATTTTCGCATTAACAATGATTTC	*Kpn*I
803	toxSDSR	GATCGAGCTCGAAATTTGGAAAAGATGACAGG	*Sac*I

804 <u>Expression analysis</u>

805	VF1133expF	CAACAAAGCGTCACTCAAAC
806	VF1133expR	CCTCTAAGCTACGTGCAATC
807	VF2042expF	CAGGTGAACAAGGTCGAG
808	VF2042expR	CCTTCTTGGCAATCACGAC
809	VFA0246expF	GGTGCAGAGTGAAGCTAATG
810	VFA0246expR	TGAACCTTCAACGGTTAGTG
811	VFA0389expF	GAACGTAGCATCAGGAGAAG
812	VFA0389expR	GTGACTTAACGCTTTGGTTTC
813	flaAexpF	GTCTGTAGGTGATGCACAAG
814	flaAexpR	CGGCTGTTAGAAGCAGATAC
815	flaCexpF	GGTGGTTCTCGTCTTCTTAATG
816	flaCexpR	TCAGCATTTACAGCCCAATC
817	flaFexpF	GGAAAGTAGGTGCAGAGAATAC
818	flaFexpR	CGTCTCACCTGACATGAATAC
819	motA1expF	CCTGCAATGGGTATGATTGG

820	motA1expR	TGAGCAATAGGGAATGCAAC
821	flgMexpF	CCAGAAACTCAAGCACCTG
822	flgMexpR	CGTTCAGGATCAACTGTGTATG
823	flrAexpF	TCGTGCAGATGTTCGTATTG
824	flrAexpR	CTGCCTTCAGCTTCCATTC
825	flrBexpF	ACCGCTCTGCAATCAAATC
826	flrBexpR	TGACATCCCTTCCCTATCAC
827	VF0157expF	CCAAATGTACGCTGGCTATC
828	VF0157expR	CCATAATCACCGCCTTCTTG
829	VF0164expF	GATTCTGCTGGTGTTGCG
830	VF0164expR	GGCAAACGTCACTGGTTAG
831	VF0165expF	GTACCAGTATGCACTTTGCC
832	VF0165expR	CGGCATCCACAACCAATAC
833	hbtRexpF	GCTGTTCCTGCAACAAGTAG
834	hbtRexpR	GAGACTACCACTTCCTGCTG
835	litRexpF	GGAGTACCTCTACTCGTG
836	litRexpR	CAGGGGTATGATCGTTAC
837	toxTexpF	AAAGAACTAGAGTCTCGAGGAG
838	toxTexpR	ACTTGGTGCTACATTCATGG
839	VCpolAqF	AAGAGCTGGCTTTGGATTAC
840	VCpolAqR	CCGTCACTGCTTGATGATAG

841 <u>*In situ* HCR probes targeting *hbtR*</u>

842 ATGGTTTTTAAACTCAATGAAATCTATTGGGATCCAGCAACAAAAAAATTGT

GATACGCTAGAAGATGCAGTTAATGGTAATAACGAATATGGTTCAACAACGC

TTAGTTTCTGCAATTCTGACTTTGTTAATAAAAGAACATCCTTCTATTTGTA

AATGAACATATTAAAGATGCTCTTTGGGGGACTCAGTGGATATCAAATGAAA

ATTCCTCAGTTAATTAAAAGAACAAGAGTATCAATAAAAGATACGAATAGAC

GTTATCGAAAATGTAAAAGGCAATGGTTATAAAATAAACAATGTAGAAGAGA

AGAATAAATTCAAATAGCATACAATGCACAGAGAAAAAAACGTCACATTCTA

TCAGCATTAATCTTTTGTATAGAAAAACATGTGTTTTACGATCTAATTCCTT

GAAGAGATAAAAAAAGTCAAAGATTTTGATTTAATTAAAATCTCTGAAGATA

TTTTTAATTAAGACTAAAGACCAAGAGTGTGAATTGAACCTTAAAAATAAAA

FIGURE LEGENDS

FIG 1 Luminescence and growth of wild-type *V. fischeri* and Δ*hbtRC* strains. The rates of (A) light production and (B) growth in SWT were measured for wild-type *V. fischeri* (○/●) and Δ*hbtRC* (□/■) carrying empty pVSV105 (open symbols) or pVSV105::*hbtRC* (closed symbols). Results represent means of three biological replicates ± one standard deviation. RLU, relative light units; Abs, absorbance.

FIG 2 Light-organ colonization competition between wild-type *V. fischeri* and chemotaxis mutant strains. Ratios of wild-type *V. fischeri* (WT) carrying a GFP-encoding plasmid (pVSV102) vs. unlabeled ΔΔΔΔ (●) or unlabeled wild-type *V. fischeri* vs. ΔΔΔΔ carrying pVSV102 (■) colonizing juvenile *E. scolopes* light organs were measured after 3 h of exposure to the inoculum followed by 21 h of incubation in sterile seawater; (▲) both datasets combined. RCI, relative competitive index of bacterial strains. Each point represents one animal. Error bars represent ± one standard deviation.

FIG 3 EPS production in wild-type *V. fischeri*, Δ*litR*, and ΔVF_0157–80 strains. EPS in supernatants of 24-h cultures grown in 0.05% casamino acids and 6.5 mM Neu5Ac was stained with alcian blue for wild-type *V. fischeri* (○/●), Δ*litR* (□/■), and ΔVF_0157–80 (△/▲) carrying empty pVSV105 (open symbols) or pVSV105::*litR* (closed symbols). Error bars represent ± one standard deviation. Abs, absorbance.*, $p<0.05$; **, $p<0.005$; ***, $p<0.0001$; n.s., not statistically significant.

FIG 4 Light-organ colonization competition between wild-type *V. fischeri* and Δ*hbtRC* strains. Ratios of (A) wild-type *V. fischeri* (WT) carrying a GFP-encoding plasmid (pVSV102) vs. Δ*hbtRC* carrying an RFP-encoding plasmid (pVSV208) or (B) wild-type *V. fischeri* carrying pVSV208 vs. Δ*hbtRC* carrying pVSV102 colonizing juvenile *E. scolopes* light organs were measured after 1 to 10 d. (C) Ratios of wild-type *V. fischeri* with chromosomal *rfp* vs. Δ*hbtRC* with chromosomal *gfp* (●) or wild-type *V. fischeri* with chromosomal *gfp* vs. Δ*hbtRC* with chromosomal *rfp* (■) in co-colonized juvenile *E. scolopes* light organs were measured after 1 d. RCI, relative competitive index of bacterial strains. Each point represents one animal. Error bars represent ± one standard deviation.

FIG 5 Expression of *hbtR* in *V. fischeri* during expulsion from *E. scolopes* light organs. Transcripts of *hbtR* (magenta, arrowheads) were detected using *in situ* HCR in *V. fischeri* cells (green) during expulsion from *E. scolopes* juvenile light organ crypts. (A) *V. fischeri* symbionts originate in the crypt, pass through the migration path (mp), and exit through the external surface pore; (A) merged image, (A’) GFP channel, (A”) *hbtR* transcript channel (Alexa 546). (B) *V. fischeri* cells (green) are expelled through the external surface pore (asterisk) into seawater 1 h after a dawn light cue; (B) a single optical slice of the superficial layer above the exit point from host and *V. fischeri* cells outside of the pore expressing *htbR*; (B’), the corresponding merged composite stack (video in Movie S1). (C) One hour after expulsion into ambient seawater, vented cells express *htbR* (magenta); enlargement is of the area within the dashed square. (C’) Percentage and 95% confidence intervals of vented cells expressing *htbR* calculated

from four samples of ventate on slides, from two experiments. Blue, *E. scolopes* nuclei (DAPI).

FIG 6 Model proposing an interactive regulation by HbtR and LitR in *V. fischeri* during colonization of and expulsion from the *E. scolopes* light organ. Upon colonization, LitR regulates relevant physiological phenotypes, including activation of luminescence and EPS production and repression of motility and chemotaxis. HbtR represses LitR upon expulsion of *V. fischeri* from the light organ, reversing this process and leading to the upregulation of motility and chemotaxis and the downregulation of luminescence and EPS production. Gray text, downregulated genes and phenotypes; blue text, upregulated genes and phenotypes.

FIG S1 Luminescence of wild-type *V. fischeri* and Δ*hbtRC* strains during symbiosis. Luminescence was measured in juvenile squid 24 h or 48 h after colonization with either wild-type *V. fischeri* (●) or Δ*hbtRC* (■). Each point represents one animal. Mean values indicated; no significant differences were noted between strains at either timepoint. RLU, relative light units.

FIG S2 Growth of wild-type *V. fischeri* and chemotaxis mutants on *N*-acetylated sugars. (A) The rates of growth in MSM supplemented with 0.05% casamino acids and 6.5 mM Neu5Ac were measured for wild-type *V. fischeri* (●), ΔΔΔΔ (■), and ΔVF_1133 ΔVF_A0246 (▲). (B) The rates of growth in MSM supplemented with 0.05% casamino

acids and 6.5 mM GlcNAc were measured for wild-type *V. fischeri* (●) and ΔΔΔΔ (■). Results represent means of three biological replicates ± one standard deviation. Abs, absorbance.

Movie S1 Expression of *hbtR* in *V. fischeri* cells during their expulsion from an *E. scolopes* light organ. *hbtR* transcripts were detected using *in situ* HCR in *V. fischeri* cells expelled from the external surface pore of the light organ 1 h after a dawn light cue. Merged stack of images depicted in Fig 5B'. Blue, *E. scolopes* nuclei (DAPI); green, *gfp*-labeled *V. fischeri*; magenta, *hbtR* transcripts labeled with Alexa 546.

FIGURES

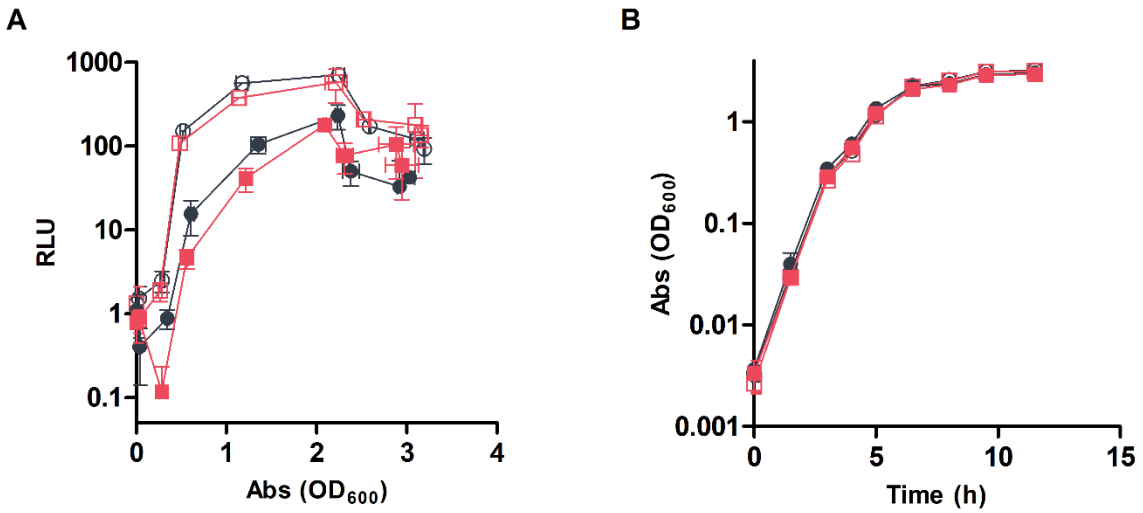

FIG 1 Luminescence and growth of wild-type *V. fischeri* and Δ*hbtRC* strains. The rates of (A) light production and (B) growth in SWT were measured for wild-type *V. fischeri* (○/●) and Δ*hbtRC* (□/■) carrying empty pVSV105 (open symbols) or pVSV105::*hbtRC* (closed symbols). Results represent means of three biological replicates ± one standard deviation. RLU, relative light units; Abs, absorbance.

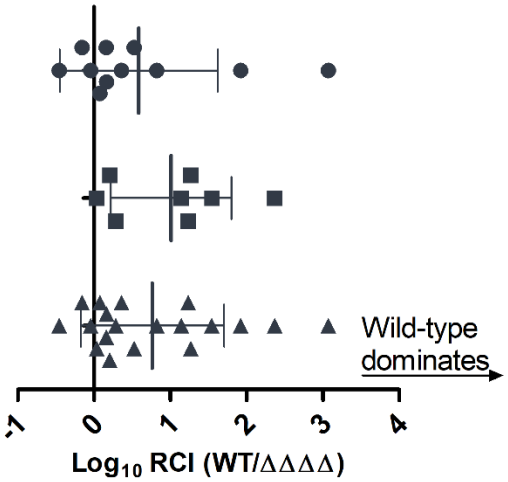

FIG 2 Light-organ colonization competition between wild-type *V. fischeri* and chemotaxis mutant strains. Ratios of wild-type *V. fischeri* (WT) carrying a GFP-encoding plasmid (pVSV102) vs. unlabeled ΔΔΔΔ (●) or unlabeled wild-type *V. fischeri* vs. ΔΔΔΔ carrying pVSV102 (■) colonizing juvenile *E. scolopes* light organs were measured after 3 h of exposure to the inoculum followed by 21 h of incubation in sterile seawater; (▲) both datasets combined. RCI, relative competitive index of bacterial strains. Each point represents one animal. Error bars represent ± one standard deviation.

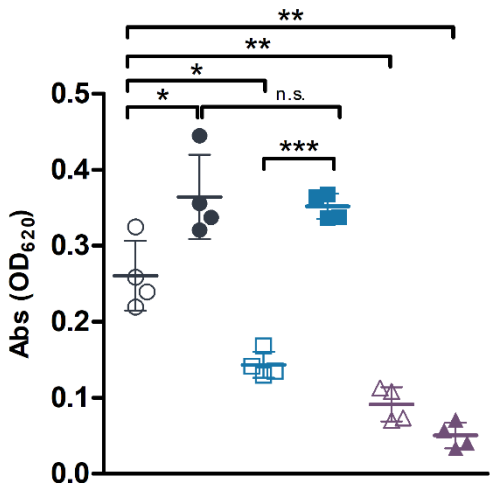

FIG 3 EPS production in wild-type *V. fischeri*, Δ*litR*, and ΔVF_0157–80 strains. EPS in supernatants of 24-h cultures grown in 0.05% casamino acids and 6.5 mM Neu5Ac was stained with alcian blue for wild-type *V. fischeri* (○/●), Δ*litR* (□/■), and ΔVF_0157–80 (△/▲) carrying empty pVSV105 (open symbols) or pVSV105::*litR* (closed symbols). Error bars represent ± one standard deviation. Abs, absorbance.*, $p<0.05$; **, $p<0.005$; ***, $p<0.0001$; n.s., not statistically significant.

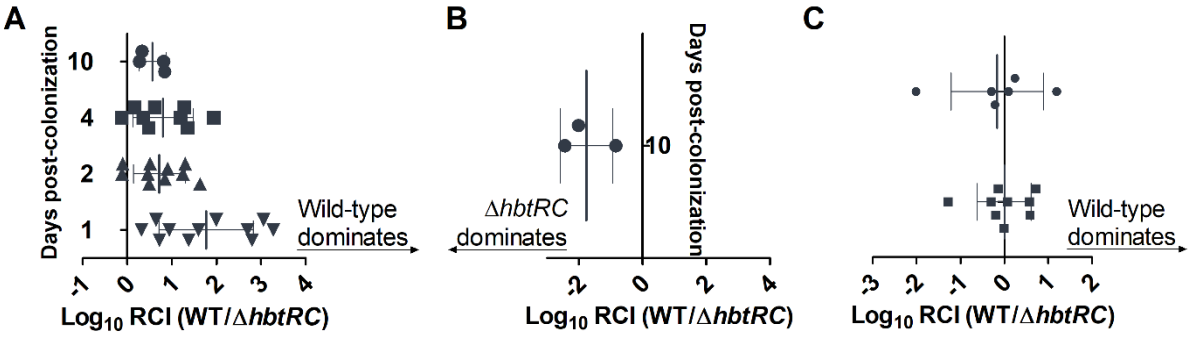

FIG 4 Light-organ colonization competition between wild-type *V. fischeri* and Δ*hbtRC* strains. Ratios of (A) wild-type *V. fischeri* (WT) carrying a GFP-encoding plasmid (pVSV102) vs. Δ*hbtRC* carrying an RFP-encoding plasmid (pVSV208) or (B) wild-type *V. fischeri* carrying pVSV208 vs. Δ*hbtRC* carrying pVSV102 colonizing juvenile *E. scolopes* light organs were measured after 1 to 10 d. (C) Ratios of wild-type *V. fischeri* with chromosomal *rfp* vs. Δ*hbtRC* with chromosomal *gfp* (●) or wild-type *V. fischeri* with chromosomal *gfp* vs. Δ*hbtRC* with chromosomal *rfp* (■) in co-colonized juvenile *E. scolopes* light organs were measured after 1 d. RCI, relative competitive index of bacterial strains. Each point represents one animal. Error bars represent ± one standard deviation.

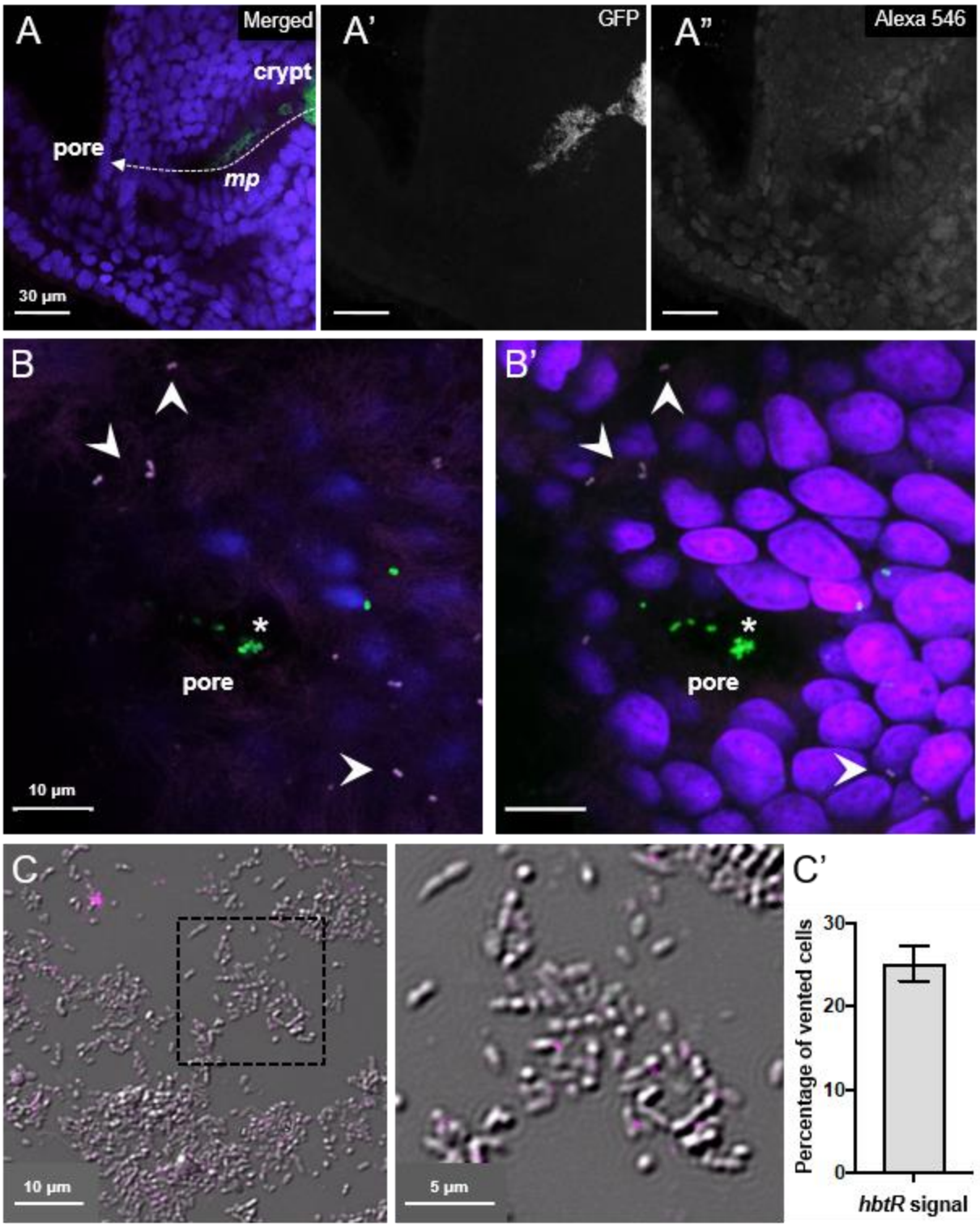

FIG 5 Expression of *hbtR* in *V. fischeri* during expulsion from *E. scolopes* light organs. Transcripts of *hbtR* (magenta, arrowheads) were detected using *in situ* HCR in *V.*

fischeri cells (green) during expulsion from *E. scolopes* juvenile light organ crypts. (A) *V. fischeri* symbionts originate in the crypt, pass through the migration path (mp), and exit through the external surface pore; (A) merged image, (A') GFP channel, (A") *hbtR* transcript channel (Alexa 546). (B) *V. fischeri* cells (green) are expelled through the external surface pore (asterisk) into seawater 1 h after a dawn light cue; (B) a single optical slice of the superficial layer above the exit point from host and *V. fischeri* cells outside of the pore expressing *htbR*; (B'), the corresponding merged composite stack (video in Movie S1). (C) One hour after expulsion into ambient seawater, vented cells express *htbR* (magenta); enlargement is of the area within the dashed square. (C') Percentage and 95% confidence intervals of vented cells expressing *htbR* calculated from four samples of ventate on slides, from two experiments. Blue, *E. scolopes* nuclei (DAPI).

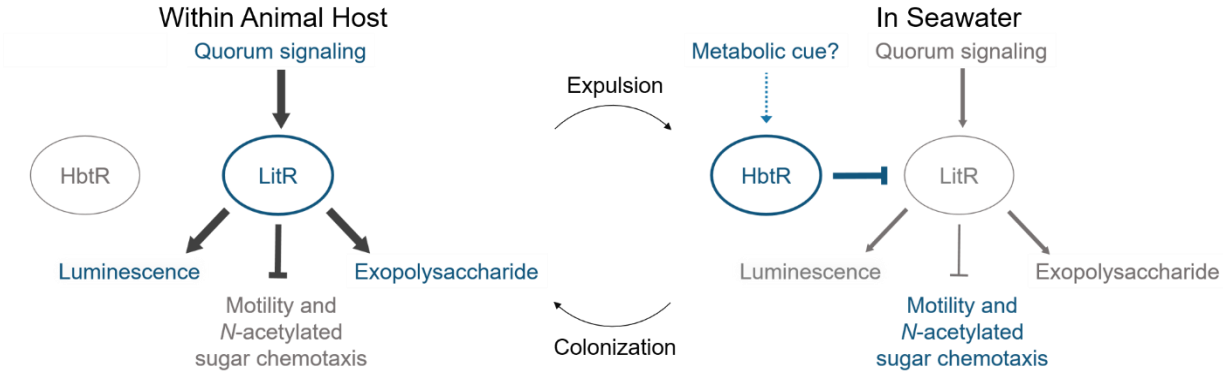

FIG 6 Model proposing an interactive regulation by HbtR and LitR in *V. fischeri* during colonization of and expulsion from the *E. scolopes* light organ. Upon colonization, LitR regulates relevant physiological phenotypes, including activation of luminescence and EPS production and repression of motility and chemotaxis. HbtR represses LitR upon expulsion of *V. fischeri* from the light organ, reversing this process and leading to the upregulation of motility and chemotaxis and the downregulation of luminescence and EPS production. Gray text, downregulated genes and phenotypes; blue text, upregulated genes and phenotypes.

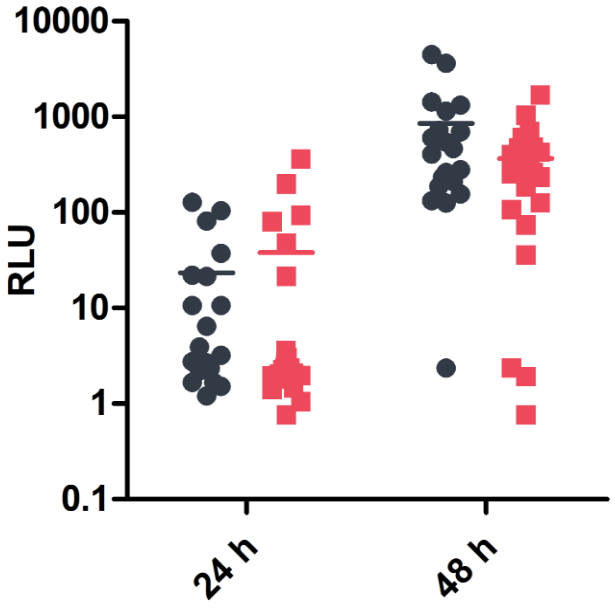

FIG S1 Luminescence of wild-type *V. fischeri* and Δ*hbtRC* strains during symbiosis. Luminescence was measured in juvenile squid 24 h or 48 h after colonization with either wild-type *V. fischeri* (●) or Δ*hbtRC* (■). Each point represents one animal. Mean values indicated; no significant differences were noted between strains at either timepoint. RLU, relative light units.

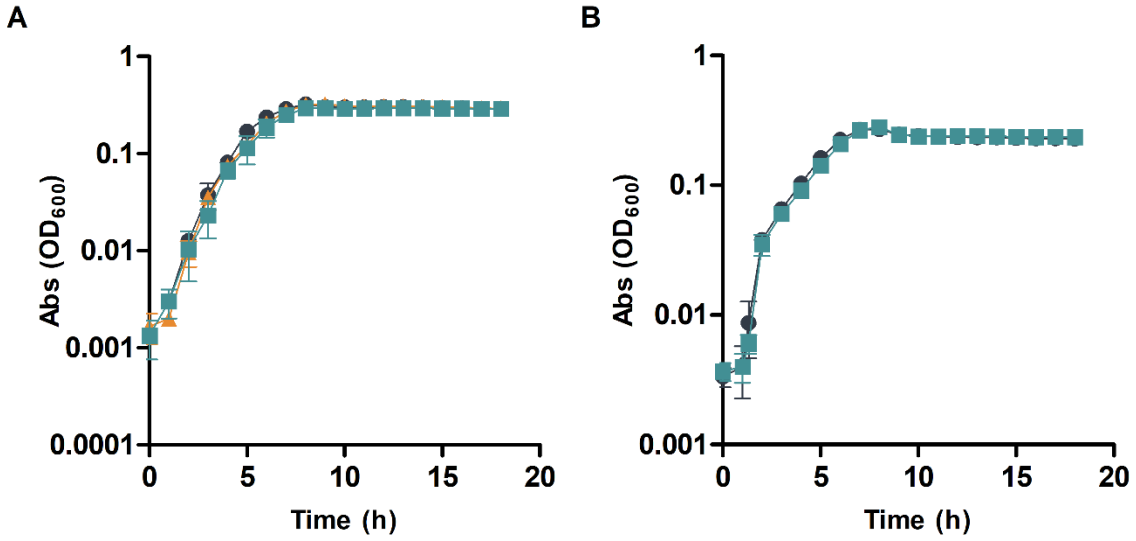

FIG S2 Growth of wild-type *V. fischeri* and chemotaxis mutants on *N*-acetylated sugars. (A) The rates of growth in MSM supplemented with 0.05% casamino acids and 6.5 mM Neu5Ac were measured for wild-type *V. fischeri* (●), ΔΔΔΔ (■), and ΔVF_1133 ΔVF_A0246 (▲). (B) The rates of growth in MSM supplemented with 0.05% casamino acids and 6.5 mM GlcNAc were measured for wild-type *V. fischeri* (●) and ΔΔΔΔ (■). Results represent means of three biological replicates ± one standard deviation. Abs, absorbance.

Movie S1 Expression of *hbtR* in *V. fischeri* cells during their expulsion from an *E. scolopes* light organ. *hbtR* transcripts were detected using *in situ* HCR in *V. fischeri* cells expelled from the external surface pore of the light organ 1 h after a dawn light cue. Merged stack of images depicted in Fig 5B'. Blue, *E. scolopes* nuclei (DAPI); green, *gfp*-labeled *V. fischeri*; magenta, *hbtR* transcripts labeled with Alexa 546.